JOURNAL OF THEORETICAL AND APPLIED MECHANICS
48, 4, pp. 1043-1056, Warsaw 2010

TWO-WAY ROTARY SHAPE MEMORY ALLOY THIN STRIP ACTUATOR

Hisaaki Tobushi

Department of Mechanical Engineering, Aichi Institute of Technology, Yachigusa, Yakusa-cho, Toyota, Japan; e-mail: tobushi@aitech.ac.jp

Elżbieta A. Pieczyska, Wojciech K. Nowacki

Institute of Fundamental Technological Research, Polish Academy of Sciences, Warsaw, Poland e-mail: epiecz@ippt.gov.pl

Kousuke Date, Kouji Miyamoto

Department of Mechanical Engineering, Aichi Institute of Technology, Yachigusa, Yakusa-cho, Toyota, Japan

In order to develop a two-way rotary shape memory alloy thin strip actuator, the torsional deformation and fatigue properties of a TiNi SMA thin strip were investigated. The results obtained are summarized as follows. (1) In the SMA thin strip subjected to torsion, the MT appears along the edge of the strip due to elongation of the edge of the strip and grows to the central part. (2) The number of cycles to failure decreases with an increase in the maximum angle of twist in torsion fatigue. The fatigue life in pulsating torsion is longer than that in alternating torsion by five times. The fatigue limit exists in a certain value of dissipated work of the strip in each cycle. (3) Based on the two-way motion of a lifting actuator model driven by two kinds of SMA thin strip, it is confirmed that the two-way rotary actuator with a small and simple mechanism can be developed by using the SMA thin strips.

Key words: shape memory alloy, thin strip, torsion, cyclic deformation, fatigue, rotary actuator, two-way motion

1. Introduction

The intelligent or smart materials having the functions of sensing, judging and working have attracted worldwide attention. One of the main materials which have activated the research on the intelligent materials is the shape

memory alloy (SMA) (Chu and Zhao, 2002; Duerig *et al.*, 1990; Funakubo, 1987; Otsuka and Wayman, 1998; Saburi, 2000). The main characteristics of SMA are the shape memory effect (SME) and superelasticity (SE). Thanks to these characteristics, SMAs are used in driving elements of actuators, heat engines and robots. In the SMAs used in practical applications, TiNi SMAs are the most widely employed, since their grain size is small and there is little risk of inducing fatigue damage; in other words, they have a high fatigue strength and a long fatigue life (Holtz *et al.*, 1999; Matsui *et al.*, 2006, 2004). The SME and SE appear as a result of the martensitic transformation (MT).

The deformation properties of the SME and SE strongly depend on temperature and stress. Because of the adaptable thermal response of SMA elements, thin wires and thin tapes are widely used in practical applications. These materials are in the market and can be obtained easily. The main loading conditions in these applications tend to be tension, compression, bending and torsion. In a recent study using the torsional deformation of a TiNi SMA tube, the twist in blades of rotor aircraft was investigated in order to improve the flight performance (Mabe *et al.*, 2004, 2007).

In practical applications making use of SMA thin strips, torsional deformation can be simply obtained by gripping both ends without any mechanical process. If the characteristics of SE are exploited, a high performance of energy storage can be achieved similar to that of a torsion bar. A large recovery torque can also be obtained under the twisted state by heating. In this way of using torsional characteristics of SMA thin strips, simple and small rotary actuators can be developed. In the case of an SMA thin strip twisted by fixing both ends, which may be employed in practical applications, not only torsional but also tensile stress can be induced along both edges of the strip. As the shearing deformation properties of the material and the thermomechanical properties under multiaxial stress states are not clear, the deformation properties of the SMA thin strip in torsion cannot be precisely estimated by the deformation properties of SMA wires and tubes which have been obtained till now. The authors investigated therefore the basic deformation properties of an SMA thin strip in torsion (Tobushi *et al.*, 2008, 2009).

In the present study, in order to develop a two-way rotary SMA thin strip actuator, the tensile deformation properties along the edge of a TiNi SMA thin strip are investigated in torsion. The cyclic torsional deformation properties, which are important in the rotary actuator, are also investigated. The fatigue properties are investigated in pulsating torsion and alternating torsion. The two-way actuator for lifting and lowering a basket driven by SMA thin strips is demonstrated.

2. Experimental method for torsional deformation

2.1. Materials and specimen

The materials used in the experiment were Ti-50.18at%Ni SMA thin strip with thickness of $t = 0.25\,\text{mm}$ and width of $w = 5\,\text{mm}$. The specimen was a uniform flat tape of length $L = 60\,\text{mm}$. The gauge length of the specimen was $l = 40\,\text{mm}$. The transformation temperatures obtained from the DSC test were $M_s = 304\,\text{K}$, $M_f = 266\,\text{K}$, $A_s = 319\,\text{K}$ and $A_f = 359\,\text{K}$.

2.2. Experimental procedure

In the torsion test, the specimen was first held by the grips and the grips were fixed on the twisting shaft. The specimen was twisted at the prescribed angle of twist per unit length θ (total angle of twist ϕ). In the cyclic torsional test, the specimen was subjected to pulsating and alternating torsion. The maximum angle of twist per unit length θ_{max} was $78.5\,\text{rad}\cdot\text{m}^{-1}$ (maximum total angle of twist $\phi_{max} = \pi$). In the torsion fatigue test, the specimen was twisted cyclically at room temperature in air at the amplitude of the prescribed angle of twist, and the number of cycles to failure was measured. The fatigue test was carried out for pulsating and alternating torsion. The frequency was 600 cpm (10 Hz).

The experimental apparatus used for the torsion test and the torsion fatigue test was presented in the previous paper (Tobushi *et al.*, 2009).

3. Experimental results and discussion for torsional deformation

3.1. Basic deformation property of the material

The stress-strain curve obtained from the tension test for the SMA thin strip at room temperature is shown in Fig. 1. The strain rate was $1.67{\cdot}10^{-5}\,\text{s}^{-1}$. Although the clear yielding phenomenon due to the MT starts at strain of 0.3%, the slope of the stress-strain curve starts to be gentle at strain of 0.2%. A residual strain of 4.8% appears after unloading. The residual strain disappears when heating occurs under no load, showing the SME. The elastic modulus determined from the slope of the initial stress-strain curve is 28 GPa.

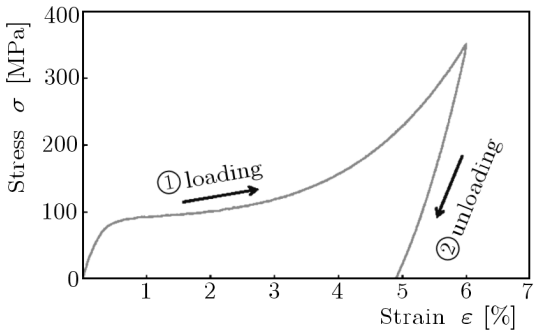

Fig. 1. Relationship between the stress and strain in tension

3.2. Torsional deformation properties

3.2.1. Twisted state

The photographs of the twisted SMA thin strip are shown in Fig. 2 for each angle of twist. The left side shows the fixed end and the right side the twisted end. The crossover point of the upper and lower surfaces of the SMA thin strip propagates from the twisting end at the angle of twist per unit length $\theta = 39.3\,\mathrm{rad{\cdot}m^{-1}}$ (total angle of twist $\phi = \pi/2$) and reaches the central part of the specimen at $\theta = 78.5\,\mathrm{rad{\cdot}m^{-1}}$ ($\phi = \pi$). We note that both edges of the thin strip are elongated by twisting since both ends are axially fixed. Therefore, tensile stress is induced along both edges, and the stress state becomes different from the simple shear and much more complex.

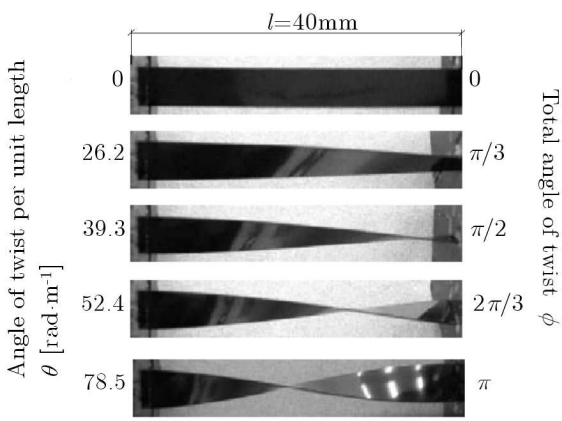

Fig. 2. Photographs of the twisted SMA thin strip at each angle of twist

3.2.2. Temperature characteristics

The thermomechanical characteristics of SMA appear due to the MT and the reverse transformation. The exothermic reaction and endothermic reaction occur based on the MT and the reverse transformation, respectively. The initiation and growth processes of the MT can be therefore analyzed by measuring temperature on the surface of the material. The infrared thermography to measure the temperature distribution on the whole surface of the material can be applied to this objective. The temperature distribution on the surface of the SMA thin strip at each angle of twist during the torsional deformation obtained by the infrared thermography is shown in Fig. 3. The maximum temperature on the surface of the specimen appears along the edge of the thin strip, and the exothermic MT occurs in this part and grows toward the central part of the specimen with an increase in the angle of twist. The temperature rise along the edge of the strip starts at the angle of twist per unit length $\theta = 13.1\,\mathrm{rad{\cdot}m^{-1}}$. The temperature increases markedly at $\theta = 26.2\,\mathrm{rad{\cdot}m^{-1}}$. Therefore, the MT grows preferentially based on the elongation along the edge of the strip.

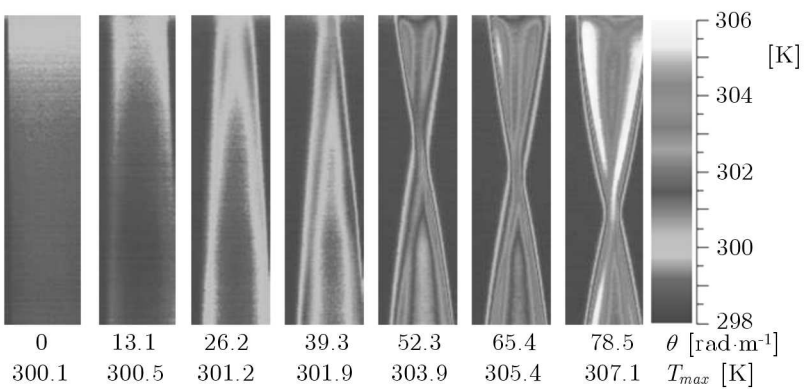

Fig. 3. Thermograms showing temperature distribution on the surface of the SMA thin strip appeared due to phase transformation during torsion

3.2.3. Elongation of the edge in a thin strip

Elongation of the edge in the SMA thin strip was measured by a thickness gauge from the gap of two thin wires pasted on the edge of the thin strip. The relationship between the tesile strain of the edge ε and the angle of twist per unit length θ is shown in Fig. 4. In contrast, the result calculated by assuming that the deformed state of the edge in the thin strip with width w

subjected to torsion is equal to helix on the surface of a column with diameter w is shown by the dashed line in Fig. 4. As can be seen, the tensile strain of the edge in the strip appears from the initial stage of twisting. The angle of twist per unit length θ corresponds to the clear MT starting strain of 0.3% is $15 \sim 30\,\mathrm{rad{\cdot}m^{-1}}$. The MT starting strain of 0.2% observed in Fig. 1 corresponds to the angle of twist per unit length less than $15\,\mathrm{rad{\cdot}m^{-1}}$. Therefore, the temperature rise along the edge of the thin strip which starts at $\theta = 13.1\,\mathrm{rad{\cdot}m^{-1}}$ (see in Fig. 3) must appear due to the MT.

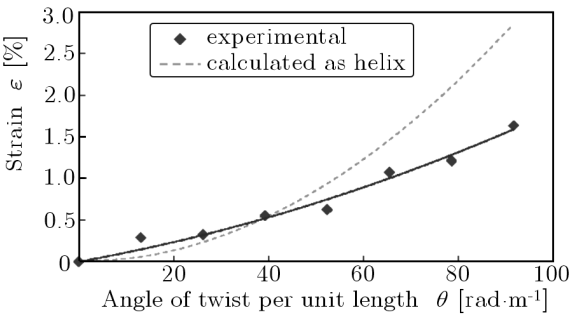

Fig. 4. Strain of the edge in the thin strip under torsion

3.3. Cyclic torsional deformation

3.3.1. Deformation in pulsating torsion

The relationships between the torque M and angle of twist per unit length θ obtained by the pulsating torsion test for the maximum angle $\theta_m = 52.4\,\mathrm{rad{\cdot}m^{-1}}$ and $78.5\,\mathrm{rad{\cdot}m^{-1}}$ are shown in Fig. 5. In the first loading process, the curve between M and θ is expressed almost by a straight line. In the unloading process, the initial slope of the curve is steep and thereafter becomes to be the plateau stage. In the reloading process, the initial curve is almost parallel to the first loading curve and thereafter the slope of the curve becomes steep. The point at the end of the reloading curve coincides with the point at which the unloading started, showing the return-point memory (Pieczyska *et al.*, 2007).

3.3.2. Deformation in alternating torsion

The relationships between the torque M and angle of twist per unit length θ obtained by the alternating torsion test for the maximum angle $\theta_m = 52.4\,\mathrm{rad{\cdot}m^{-1}}$ and $78.5\,\mathrm{rad{\cdot}m^{-1}}$ are shown in Fig. 6. Compared with

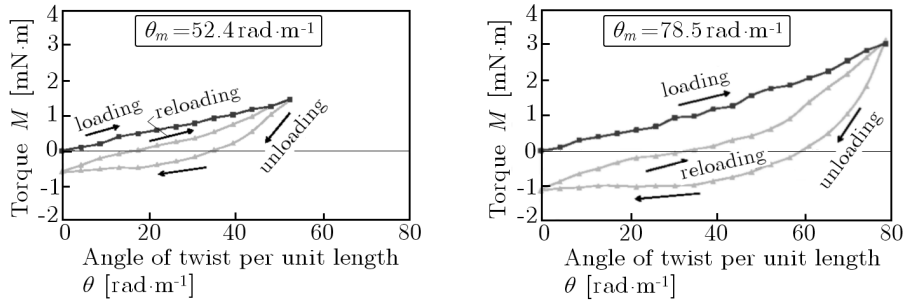

Fig. 5. Relationship between the torque M and angle of twist per unit length θ obtained by the pulsating torsion test

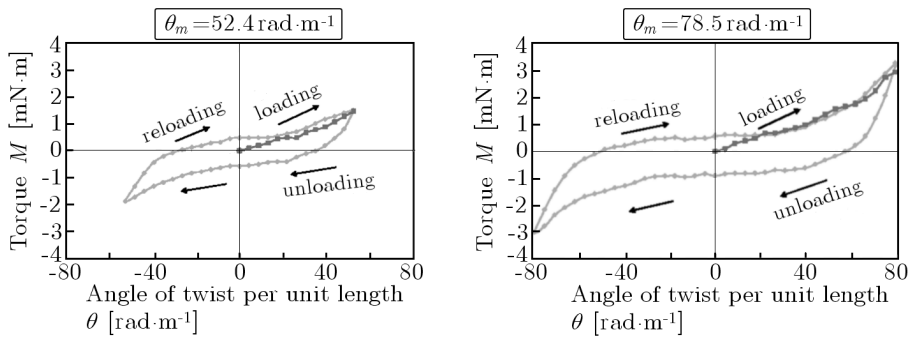

Fig. 6. Relationship between the torque M and angle of twist per unit length θ obtained by the alternating torsion test

the pulsating torsion shown in Fig. 5, the twisting in the reverse direction to the first twisting direction was carried out. The reverse loading and unloading curves are almost similar to the first loading and unloading curves except for the early stage. That is, the first and reloading curves are closely symmetric with respect to the origin. In the reloading process, the inital slope of the unloading curve is steep and the plateau stage appears thereafter. The point at the end of the reloading curve almost coincides with the point at which the first unloading started, showing the return-point memory, the same as in the pulsating torsion.

3.3.3. Torsional rigidity

In the elastic deformation of torsion, the relationship between the increments of torque ΔM and angle of twist per unit length $\Delta\theta$ is given by the following equation

$$\Delta\theta = \frac{\Delta M}{k} \tag{3.1}$$

where k denotes the torsional rigidity. In the case of a circular bar, $k = GI_p$ where G and I_p represent the modulus of rigidity and polar area moment of inertia, respectively. In the case of a bar of narrow rectangular cross section, $k = wt^3G/3$, where w and t denote the width and thickness, respectively (Timoshenko and Goodier, 1982). We note that axial stress and strain are assumed to be zero in these cases. In the present study, considering practical application of the thin strip to a rotary driving element, both ends are axially fixed, and therefore both edges of the strip are elongated by twisting as observed in Figs. 3 and 4. That is, the axial stress and strain appear during twisting the thin strip, and the assumption of no axial stress and strain does not hold.

The relationship between the torque M and angle of twist per unit length θ in alternating twisting with $\theta_m = 52.4\,\mathrm{rad{\cdot}m^{-1}}$ is shown in Fig. 7. In Fig. 7, the slopes in the early stage of the loading and unloading curves are denoted by k_l and k_u, respectively. The average values of k_l and k_u obtained at various maximum angles θ_m are $3 \cdot 10^{-5}\,\mathrm{N{\cdot}m^2}$ and $2.5 \cdot 10^{-4}\,\mathrm{N{\cdot}m^2}$.

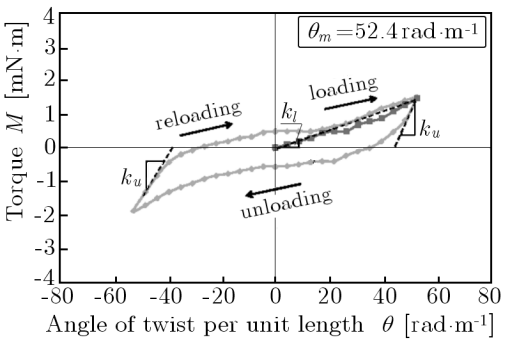

Fig. 7. Relationship between the torque and angle of twist per unit length in alternating twisting with $\theta = 52.4\,\mathrm{rad{\cdot}m^{-1}}$

The calculated result of $k = wt^3G/3$ for $w = 5\,\mathrm{mm}$, $t = 0.25\,\mathrm{mm}$ and $G = 10\,\mathrm{GPa}$ is $2.6 \cdot 10^{-4}\,\mathrm{N{\cdot}m^2}$. The calculated torsional rigidity k is close to the initial slope of the unloading curve k_u. Therefore, we should note that Eq. (3.1) with $k = wt^3G/3$ can not be applied to the evaluation of the loading curve but can be applied to the evaluation of the unloading curve in the early stage.

3.3.4. Dissipated work

The area surrounded by the hysteris loop of the torque-angle curve of twist shown in Figs. 5 and 6 expresses the dissipated work per unit length W_d.

The relationships between the dissipated work per unit length W_d and the maximum angle of twist per unit length θ_m obtained by the pulsating and alternating torsion tests are shown in Fig. 8. The dissipated work W_d increases in proportion to the maximum angle of twist θ_m. The value of W_d in the alternating torsion is larger than that in the pulsating torsion by 3.5 times. W_d is very small if θ_m is smaller than a certain value in both alternating and pulsating torsion.

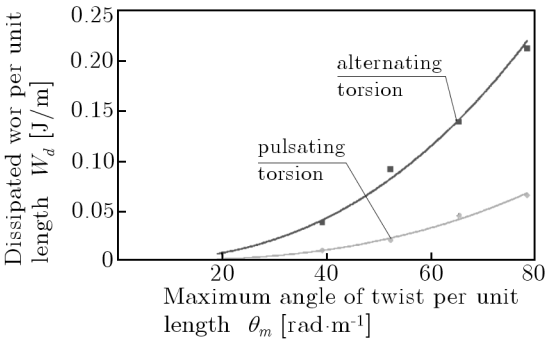

Fig. 8. Relationship between the dissipated work and maximum angle of twist per unit length

3.4. Torsion fatigue properties

The relations between the maximum angle of twist per unit length θ_m and the number of cycles to failure N_f obtained from the torsion fatigue test are shown in Fig. 9. As can be seen in Fig. 9, the number of cycles to failure N_f decreases with an increase in the maximum angle of twist per unit length θ_m in the region of low-cycle fatigue. This relation is approximated by a straight line on the logarithmic graph. The fatigue life curve seems therefore to be expressible in an equation similar to that for TiNi SMA wires under bending. This can be seen in Eq. (3.2)

$$\theta_m N_f^{\beta} = \alpha \tag{3.2}$$

$$\begin{cases} \beta = 0.1, & \alpha = 265\,\mathrm{rad}\cdot\mathrm{m}^{-1}: \quad \text{Pulsating torsion} \\ \beta = 0.13, & \alpha = 310\,\mathrm{rad}\cdot\mathrm{m}^{-1}: \quad \text{Alternating torsion} \end{cases}$$

where α and β represent θ_m where $N_f = 1$ and the slope of the $\log\theta_m - \log N_f$ curve, respectively. The calculated results obtained from Eq. (3.2) are shown by the solid lines in Fig. 9. As can be seen, the low-cycle fatigue life curves are well matched by the solid calculation lines.

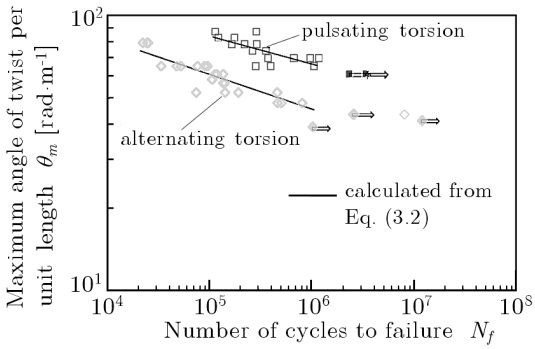

Fig. 9. Fatigue-life curves of the SMA thin strip for the alternating and pulsating torsion

Comparing the fatigue life of alternating torsion and pulsating torsion, the number of cycles to failure N_f for alternating torsion is smaller than that for pulsating torsion by 1/5. As observed in Fig. 8, the dissipated work W_d in the alternating torsion is larger than that in the pulsating torsion by 3.5 times. The fatigue damage due to the dissipated work is therefore larger in the alternating torsion, resulting in shorter fatigue life.

The maximum angle of twist per unit length θ_m for the fatigue limit at which the fatigue life curve becomes horizontal is $44\,\mathrm{rad{\cdot}m^{-1}}$ for the alternating torsion and $61\,\mathrm{rad{\cdot}m^{-1}}$ for the pulsating torsion, respectively. The dissipated work W_d in each cycle which corresponds to the fatigue limit of the maximum angle of twist per unit length θ_m is obtained from Fig. 8. The dissipated work W_d at $\theta_m = 44\,\mathrm{rad{\cdot}m^{-1}}$ in the alternating torsion is $0.05\,\mathrm{J/m}$ and that at $\theta_m = 61\,\mathrm{rad{\cdot}m^{-1}}$ in the pulsating torsion is $0.04\,\mathrm{J/m}$. Therefore, the dissipated work corresponding to the fatigue limit must exist at 0.04-0.05 J/m. If the dissipated work in each cycle is smaller than 0.04-0.05 J/m, the fatigue damage is slight, resulting in long fatigue life.

4. Two-way rotary actuator model

If an SMA thin strip is heated by keeping the twist angle constant, the recovery torque appears. Therefore, if the SMA thin strip is combined with a superelastic-SMA thin strip as a bias element, a two-way rotary actuator can be developed. In the previous paper (Tobushi *et al.*, 2009), a rotary actuator model for opening and closing the door was demonstrated. The axes of two kinds of SMA thin strips showing the SME (SME-SMA strip) and the SE at

room temperature (SE-SMA strip) were arranged in the same line in the model. In the present paper, a new rotary actuator model in which the axes of two kinds of SMA thin strips are arranged in parallel is demonstrated.

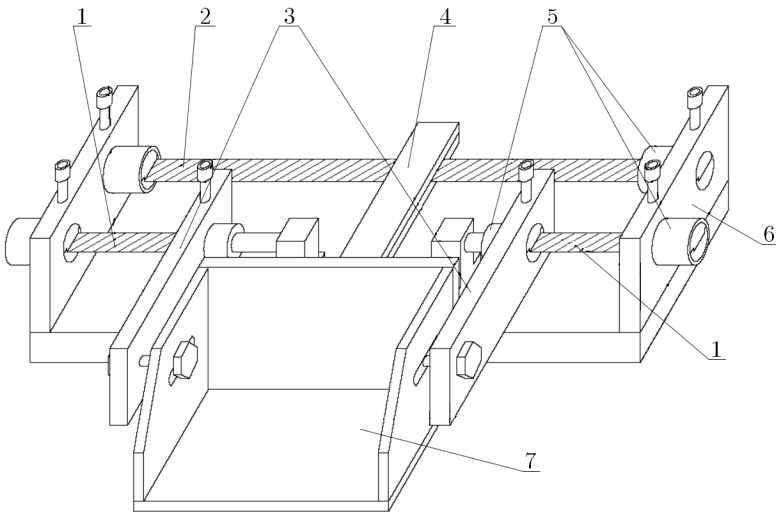

Fig. 10. Structure of the actuator for lifting and lowering a basket with two kinds of SMA thin strips; 1 – SME-SMA thin strip, 2 – SE-SMA thin strip, 3 – arm, 4 – center bar, 5 – grip, 6 – side body, 7 – basket

The structure of the two-way actuator for lifting and lowering a basket driven by the SMA-thin strips under heating and cooling is shown in Fig. 10. The principle and photographs of two-way motion of the actuator are shown in Figs. 11 and 12, respectively. The SME-SMA thin strip is the same as the TiNi SMA specimen used in the present study. The SE-SMA strip with thickness of $t = 0.25\,\mathrm{mm}$ and width of $w = 2.5\,\mathrm{mm}$ was a TiNi SMA thin strip. In the initial state, the SE-SMA strip was mounted to be in a flat plane and the SME-SMA strip was mounted at the total angle of twist $\phi = \pi/2$.

The SME-SMA strip was heated by the joule heat through an electric current. The basket was horizontal in the initial state. Since the recovery torque appeared in the SME-SMA strip by heating it, the basket moved upward. When the SME-SMA strip was cooled, the SE-SMA strip recovered the flat plane, which resulted in lowering the basket.

Thus, if two kinds of SMA thin strips which show the SME and SE are used, the two-way rotary actuator with a small and simple mechanism can be developed.

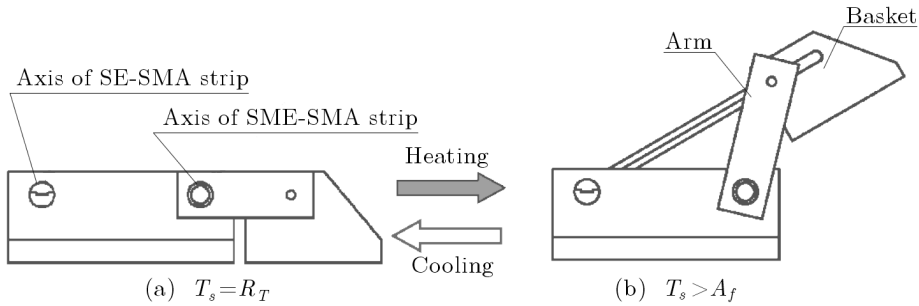

Fig. 11. Principle of the model of the actuator for lifting and lowering the basket driven by SMA-thin strips; T_s – temperature of SME-SMA strip, A_f – reverse transformation finish temperature, R_T – room temperature

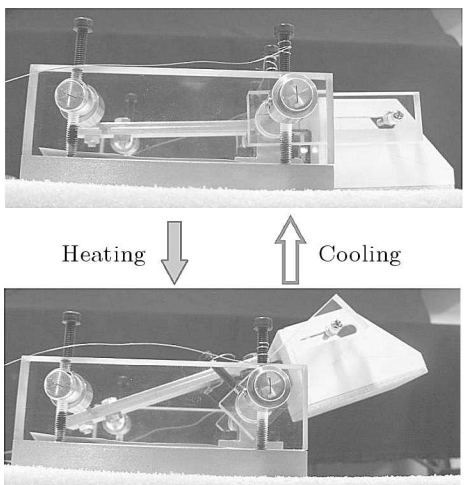

Fig. 12. Photographs of two-way motion of the actuator for lifting and lowering the basket

5. Conclusions

In order to develop the two-way rotary SMA thin strip actuator, the torsional deformation and fatigue properties of a TiNi SMA thin strip and the two-way rotary actuator model were investigated. The results obtained can be summarized as follows.

- In the SMA thin strip subjected to torsion, the MT appears along the edge of the strip due to elongation of the edge of the strip and grows to the central part.
- The number of cycles to failure decreases with an increase in the maximum angle of twist in torsion fatigue. The fatigue life in pulsating torsion

is longer than that in alternating torsion by five times. The fatigue limit exists in a certain value of disspated work of the strip in each cycle.

- Based on the two-way motion of the lifting actuator model driven by two kinds of SMA thin strips, it is confirmed that the two-way rotary actuator with a small and simple mechanism can be developed by using the SMA thin strips.

Acknowledgements

This study was performed as a part of the bilateral joint research project between Aichi Institute of Technology and Institute of Fundamental Technology Research, Polish Academy of Sciences supported by the Japan Society for Promotion of Science and Polish Academy of Sciences. The experimental work for this study was carried out with the assistance of students from Aichi Institute of Technology, to whom the authors wish to express their gratitude. The authors are also grateful to the administrators of Scientific Research (C) (General) in Grant-in-Aid for Scientific Research by the Japan Society for Promotion of Science for financial support.

References

1. Chu Y.Y., Zhao L.C., eds., 2002, Shape memory materials and its applications, *Trans. Tech. Pub.*, 177-284
2. Duerig T.W., Melton K.N., Stockel D., Wayman C.M., eds., 1990, *Engineering Aspects of Shape Memory Alloy*, Butterworth-Heinemann, 1-35
3. Funakubo H., ed., 1987, *Shape Memory Alloys*, Gordon and Breach Science Pub., 1-60
4. Holtz R.L., Sadananda K., Imam M.A., 1999, Fatigue thresholds of TiNi alloy near the shape memory transition temperature, *Int. J. Fatigue*, **21**, 137-145
5. Mabe J.H., Calkins F.T., Ruggeri R.T., 2007, Full-scale flight tests of aircraft morphing structures using SMA actuators, *Proccedings of SPIE*, 6525-65251C, 1-12
6. Mabe J.H., Ruggeri R.T., Rosenzweig E., Yu C.J., 2004, NiTinol performance characterization and rotary actuator design, *Smart Struct. Mater., Proccedings of SPIE*, **5388**, 95-109
7. Matsui R., Makino Y., Tobushi H., Furuichi Y., Yoshida F., 2006, Influence of strain ratio on bending fatigue life and fatigue crack growth in TiNi shape-memory alloy thin wires, *Mater. Trans.*, **47**, 3, 759-765

8. MATSUI R., TOBUSHI H., FURUICHI Y., HORIKAWA H., 2004, Tensile deformation and rotating-bending fatigue properties of a highelastic thin wire, a superelastic thin wire, and a superelastic thin tube of NiTi alloys, *Trans. ASME, J. Eng. Mater. Tech.*, **126**, 384-391

9. OTSUKA K., WAYMAN C.M., EDS., 1998, *Shape Memory Materials*, Cambridge University Press, 1-49

10. PIECZYSKA E.A., TOBUSHI H., NOWACKI W.K., GADAJ S.P., SAKURAGI T., 2007, Subloop deformation behavior of TiNi shape memory alloy subjected to stress-controlled loadings, *Mater. Trans.*, **48**, 10, 2679-2686

11. SABURI T., ED., 2000, Shape memory materials, *Trans. Tech. Pub.*, 315-366

12. TIMOSHENKO S.T., GOODIER J.N., 1982, *Theory of Elasticity*, 3rd ed., McGraw-Hill, 307-313

13. TOBUSHI H., PIECZYSKA E.A., NOWACKI W.K., SAKURAGI T., SUGIMOTO Y., 2009, Torsional deformation and rotary driving characteristics of SMA thin strip, *Arch. Mech.*, **61**, 3-4, 241-257

14. TOBUSHI H., SAKURAGI T., SUGIMOTO Y., 2008, Deformation and rotary driving characteristics of a shape-memory alloy thin strip element, *Mater. Trans.*, **49**, 1, 151-157

Skrętny siłownik taśmowy zaprojektowany na bazie dwukierunkowego efektu pamięci kształtu

Streszczenie

W pracy zbadano termomechaniczne właściwości skręcania i zmęczenia stopu TiNi z pamięcią kształtu (SMA) w celu zbudowania skrętnego siłownika taśmowego zaprojektowanego na bazie dwukierunkowego efektu pamięci kształtu. Otrzymane wyniki podsumowano w sposób następujący. (1) W cienkich taśmach SMA poddawanych skręcaniu, przemiana martenzytyczna (MT) inicjuje się na krawędzi taśmy w związku ze składową rozciągania, a następnie rozwija w kierunku jej środka. (2) W badaniach zmęczeniowych ilość cykli do zniszczenia maleje wraz ze wzrostem maksymalnego kąta skręcania. Wytrzymałość na zmęczenie w przypadku skręcania pulsującego jest pięciokrotnie dłuższa niż w przypadku obciążania symetrycznego. (3) Przeprowadzone badania dwukierunkowego ruchu na zaprojektowanym modelu siłownika poruszanego przy pomocy dwóch rodzajów cienkiej taśmy SMA potwierdziły możliwość zbudowania skrętnego siłownika z małym i prostym mechanizmem na bazie dwukierunkowego efektu pamięci kształtu.

Manuscript received February 17, 2010; accepted for print March 18, 2010